Contents lists available at ScienceDirect

Environmental Challenges

journal homepage: www.elsevier.com/locate/envc

Hydraulic conductivity and geophysics (ERT) to assess the aquifer recharge capacity of an inland wetland in the Brazilian Savanna

César Augusto Moreira [a,*], Vania Rosolen [a], Lucas Moreira Furlan [a], Renata Cristina Bovi [b], Henri Masquelin [c]

[a] São Paulo State University (Universidade Estadual Paulista), Department of Geology, Av. 24A, 1515, CEP, Rio Claro (SP) 13506-900, Brazil
[b] "Luiz de Queiroz" College of Agriculture, University of São Paulo (USP/ESALQ), Soil Science Department, Pádua Dias, Avenue 11, CEP, Piracicaba (SP) 13418-900, Brazil
[c] Facultad de Ciencias, Universidad de la República, Montevideo, Departamento de Montevideo, Uruguay. Iguá 4225. 11400, Montevideo, Uruguay 598-2 525-8618, Brazil

ARTICLE INFO

ABSTRACT

The inland wetlands can perform the storage of water on the surface and the recharge of aquifers. Even a small wetland can work as a local point of water infiltration, influencing and sustaining the hydrodynamics in the hydrology landscape. These zones have complex mechanisms, as they integrate soil chemical and physical characteristics, and relate both surface and groundwater systems. The study area is an inland wetland located in the Ecological Station of Itirapina, São Paulo State (Brazil). The present work aims to unveil the relationship between hydrodynamics and pedological architecture through a detailed study that combines hydraulic conductivity tests in situ, geophysical method of electrical resistivity (Electrical Resistivity Tomography technique, ERT), and morphological soil descriptions aiming the validation of the ERT and hydraulic conductivity surveys. Two-dimensional (2D) and pseudo-three-dimensional (3D) ERT have been used to investigate the water flow in the subsurface, the pedological architecture that keeps the wetland hydroperiods, and the link between surface water and groundwater that can set a recharge capacity. The results showed areas with distinct surface patterns related to the density of vegetation cover and water infiltration. The lower infiltration areas are characterized by the presence of a perched water table in grassy areas while higher infiltration is associated with exposed topsoil. ERT 2D and pseudo-3D identified these areas as zones with a connection between soil-water and groundwater systems. Hydrodynamics in the flat plateau is associated with the geochemical evolution of soil cover due to the structural complexity acquired by the iron crust dissolution (laterite) which has sustained the relief. Future studies concerning inland wetlands need to be carried out to certify the role of soil-landscape in the water cycle in the Savanna biome.

1. Introduction

Flat plateaus corresponding to paleosurfaces are typical reliefs in the Savanna biome (Migón 2004). The Depressão Periférica Paulista (Paulista Peripheral Depression, São Paulo State, Brazil) is a geomorphological compartment bordered by a sector of Cuestas with flattened tops, constituting the highland erosive surfaces of approximately 700 m a.s.l. rising above sedimentary convex hills (500–600 m a.s.l). The boundary between the compartments has been retreated by dissection caused by the modern drainage system. On the surface, the development of a network of shallow waterlogged topographic depressions has also dissected the relief, indicating the development of zero-order basins that flow towards the plateau border, possibly connected to river channels by subsurface flow. The hydroperiod is closely influenced by the rain regime, flooding during the rainy season and drying out during the dry season (Junk et al., 2014). These features correspond to inland natural wetlands and play a fundamental role to regulate water flow and provide ecosystem services (Whigham and Jordan 2003).

Even small wetlands can work as local points of water infiltration, connecting soil-water to groundwater in a local and regional hydropedological framework (van der Kamp and Hayashi 1998; Winter 1999). In the past decades, several studies demonstrated the importance to characterize wetlands' hydrology based on the intrinsic and complex relationship between soil and water to ensure local and regional water availability, combining distinct approaches and analyzing a set of parameters obtained from soil surface to saprolite in vertical and lateral

scales (Carter 1986; Mc Laughlin et al. 2014; Fleischmann et al., 2018; Lee et al., 2018; Sonkamble et al., 2019).

A previous study carried out in the flat plateau of the Brazilian Savanna showed that the connection between surface water and aquifer occurred through the opening of a leak point in the center of wetland after deferruginization of a former duricrust (Furlan et al., 2020). The process is driven by greater moisture conditions, which have altered the direction of pedogenesis, transforming the thick duricrust in a concretionary and permeable level in the soil, deepening land surface and promoting flooding by rainwater accumulation, and bringing the topographic level close to the higher water table level (Rosolen et al., 2019, Coelho et al. 2020). In the area of this study (Itirapina municipality), wetlands develop in quatz-sandy soil from Botucatu sandstone deposited in the Jurassic-Cretaceous arid environment over Serra Geral basaltic rocks (Milani et al., 1998). Corresponds to a protected area (Itirapina Ecological Station), containing the remnants of open woody and grassland savanna, some portions with periodic soil waterlogging grassland, surrounded by pinus plantation and agriculture. The soil-water availability provided by the shallow water table is the main factor in defining the vegetation dynamics, hamper the growth and survival of most tree species (Leite et al., 2018). We assumed that this remnant is a fragment that represents the former landscape and the plateau could present a set of environmental conditions that have been preserved along the time, especially when compared to the surroundings intensive land conversion to agriculture, planted forest, and urban areas.

The genesis of natural inland isolated wetlands in the region is still unknown as well as their contribution to aquifer recharge and water flow throughout the plateau. To unveil the water path, we applied geophysical Electroresistivity (Electrical Resistivity Tomography technique, ERT), a non-invasive method that provides indirect physical measures to assess the whole regolith including fluids, such as water, oil, and gas (Telford et al., 1990; Mussett and Khan 2000). Particularly, the ERT technique is suitable for hydrogeological studies due to high variability in electrical properties related to different levels of wetness or water saturation in heterogeneous soil or rock matrices and horizons. This sensitivity enables diagnoses of aquifer systems and studies of the behavior of water in recharge and discharge systems contained in porous or fractured substrates (Bower et al. 2002; de Vries and Simmers 2002;(Hiscock, 2005) Mawer et al., 2016; Sendrós et al., 2020).

Evaluate soil-water flow and its relationships with aquifer recharge-discharge is particularly useful in this region since have been occurring a growing demand for water resources related to the expansion of agriculture in the Cerrado biome (Brannstrom et al., 2008; Alho and Martins 1995; Sano et al., 2010; Jepson et al., 2010; Salazar et al., 2015). Since wetlands are a critical ecosystem and have a fundamental role in the water supply chain, the knowledge of their spatial extent and physical attributes are crucial to help implement policies prioritizing water conservation and environmental management (Fryirs et al., 2019). Therefore, unveil the water flow inside and outside inland wetlands and the interaction with aquifer and rivers has potential positive impacts on water management in a landscape deeply disturbed by human activities. Intensive land use has substantially altered the ecological function of the Cerrado landscape, highlighting imbalances in the hydrological cycles, such as in aquifer recharge and river inflow (Farley et al., 2005; Nan et al., 2011; Nosetto et al., 2012).

The objective of this study is to assess the hydrogeology of an inland natural wetland developed in a remnant of the Brazilian Savanna surrounded by intensive agriculture. Although this study was carried out on a local scale, the results could be transposed to other humid areas developed on the plateau, and it is particularly important because the Botucatu and Pirambóia formations are the two most important for the recharge of the Guarani Aquifer. The results can contribute to the discussion about the genesis and evolution of the wetlands on the surface of the flat plateau and their function in the surface water storage and groundwater interactions.

2. Material and methods

2.1. Study area

The studied area is located inside the Ecological Station of Itirapina (IES), central-eastern region of the São Paulo State, Brazil (Fig. 1). The IES is managed by the Forest and Experimental Stations Division of the Federal Forestry Institute and comprises 2300 ha intended for conservation of natural resources and scientific research (iflorestal.sp.gov.br/itirapina).

The climate of the study region is classified as Cwa according to Köppen's climate classification. It has high rainfall in summer (from October to March) and dries in winter (from April to September). It presents an average annual rainfall of 1500 mm and an average annual temperature of 21.9 °C (Troppmair 2000). Regarding hydrography, the area is drained by the Jacaré-Guaçu River sub-basin, formed by the Itaqueri and Feijão streams.

The natural vegetation of the IES is characteristic of the Savanna, with wetlands covering 29% of the station. The plateau is a segment of the Cuesta sector (Campo Alegre Plateau), from 600 to 750 m a.s.l., showing flattened and slightly dissected top hills and dissected border (Almeida 1964).

The plateau is formed by the erosion of the Botucatu Formation characterized by very fine to medium-grained reddish sandstones commonly exhibiting iron oxide film surrounding the grains. The deposition is related to a dry-eolian system, formed by sets of cross-bedded, planar cross-bedded, and low angle cross-stratification of medium and large scale ((Schneider et al., 1974)), from the terminal Jurassic to the initial Cretaceous (Milani et al., 1998). This geological unit is the main water storage and transmission compartment of the Guaraní Aquifer System (GAS), consisting of sandstones from the Pirambóia Formation at the base and Botucatu at the top.

The soils in the IES are represented by Arenosols, Ferrasols, and Gleysols with a level of iron concretion (Zanchetta et al. 2006). The Arenosols occupy the highest and well-drained relief positions and Gleysols are present in hydromorphic topographic depressions (Zanchetta et al., 2006).

The studied wetland is a closed depression with 100 m in diameter and 1 m depth in its center. Correspond to a segment of a shallow concavity network covered by grass and surrounded by open Savanna, which extends to the borders of the plateau. The wetland is saturated throughout the rainy season and in part of the dry season. In dry periods, the water table level decrease and the surface soil become dry.

Also, during the dry periods, the grassland cover diminishes in area, and patches of a dry, clean, and white sand appears among clumps of grass and some shrubs. Even during the rainy season (October-March), the vegetation cover does not reach the totality of the soil surface in reason of the low nutritional level or excess of water (Leite et al., 2018). Laterally, from the border of the wetland toward the well-drained plateau, the open Savanna dominates (Figs. 1A, 3B, 3C). Downslope, where the river channel appears, vegetation cover is composed of riparian forest (Fig. 1D and 3E).

2.2. Field studies

The fieldwork involved hydraulic conductivity in situ tests, geophysical survey using electrical resistivity tomography (ERT), and soil sampling analysis (Fig. 2).

2.2.1. Geophysical survey

The geophysical survey was performed to understand the relationship of the wetland with the local groundwater dynamic. The method applied in this study was Electroresistivity, using the technique of Electrical Resistivity Tomography (ERT).

The geophysical equipment used was the resistivimeter Terrameter LS, manufactured by ABEM Instrument Sweden, available on the Geo-
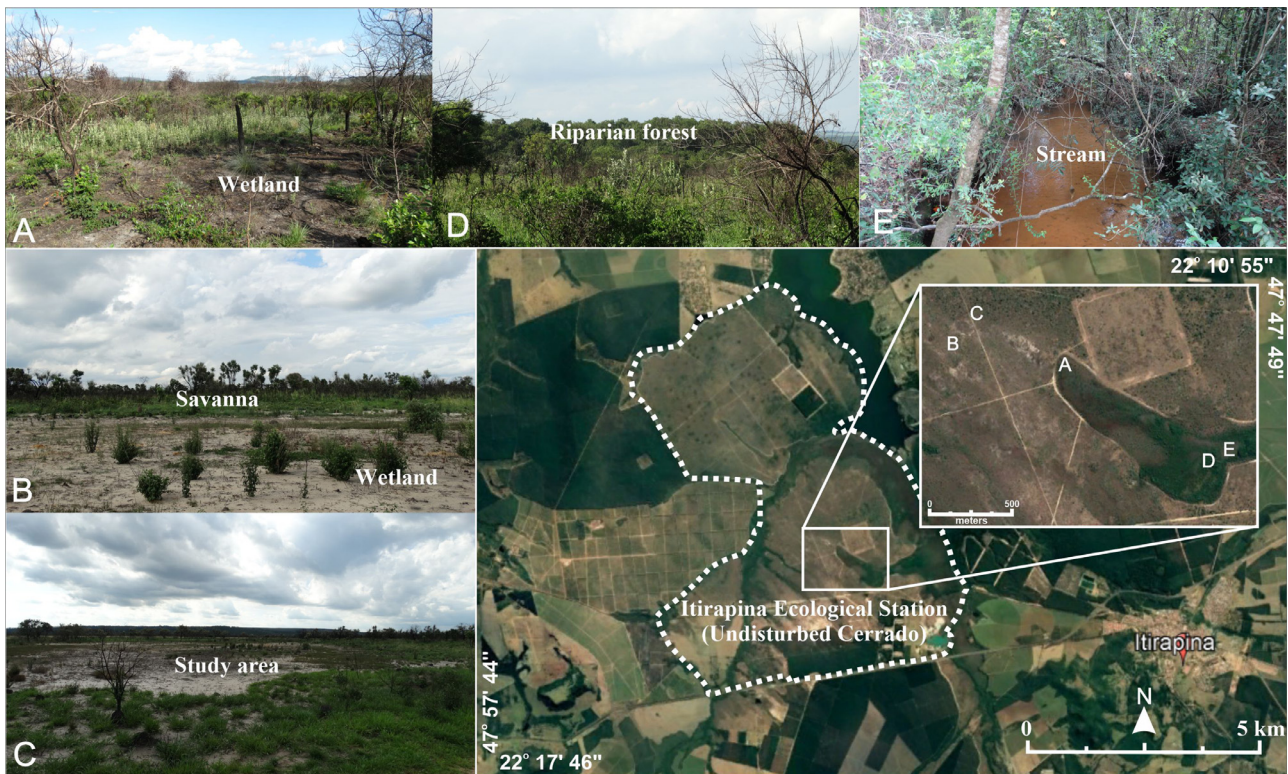
Fig. 1. Location and morphological compartments of the study region: A) Area covered by grass inside wetland; B) Area with exposed soil inside wetland and the contact wetland- open savanna; C) general view of wetland surface pattern; D and E) Riparian forest and stream located downslope of wetland systems.
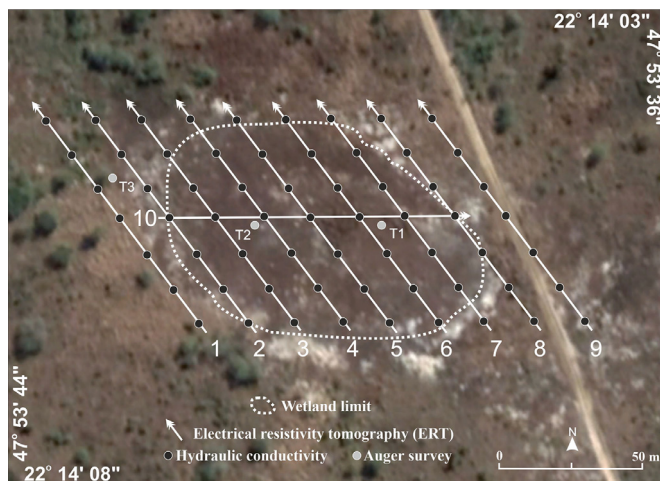

Fig. 2. ERT lines position and acquisition direction in white color, with hydraulic conductivity measure points in black, and auger investigations points in gray. The dashed line highlights the wetland limit boundary.

physics Laboratory of the Geology Department of the São Paulo State University (UNESP). The device is connected to a battery and consists of a model of transmission and reception of the signal, with the power of 250 W, resolution of 1 μV, and maximum current of 2.5 A (ABEM 2012). Cables are plugged into the device and connected by claws to the iron electrodes embedded in the ground.

In the present study, the electrode array used was the Schlumberger configuration, which presents a symmetrical arrangement of the electrodes (ABMN) in relation to a central point (resistivimeter). Electrodes (AB) are external and the potential electrodes (MN) are internal. This array is relevant in terms of the resolution of layers with a horizontal

structure, satisfactory vertical resolution, and the sensitivity to side effects close to the surface is reduced (Lowrie 2007).

The data processing was carried out in Res2dinv software (Geotomo Software 2003), designed to invert large data sets (with about 200–100,000 data points to automatically generate a two-dimensional (2D) resistivity model for the subsurface (Dahlin 1996). The Res2dinv uses the smoothed inversion routine based on the smoothness-constrained least-squares method (Loke 2004).

Next, a modeling subroutine was used to calculate the apparent resistivity values, and a non-linear least-squares optimization technique is used for the repeated inversion routine for calculating resistivity. The resistivity values are presented on a logarithmic scale, which extrapolates and highlights the contrasts. These interpolation intervals are organized on a color scale (Loke and Barker 1996). The 2D inversion data is plotted on a spreadsheet to obtain the pseudo-3D visualization models. The spreadsheet must contain the variables, x - geographic position of the readings along the acquisition lines, y - spacing between lines, z - depth by inversion, and R - resistivity value.

The pseudo-3D model is generated on the Oasis Montaj platform, in which the 2D inversion models are interpolated through the minimum curvature method. A pseudo-3D visualization model allows cuts by depth levels. In these depth models, it is possible to visualize areas with complex geological structures and particularly hydrology, as they highlight the level of soil saturation, preferential flow paths, aquifer geometry, and hydraulic properties, important information used in the design of conceptual models of hydrogeological systems. This methodology has already been used in other studies related to hydrogeology at the same biome or geology (Robineau et al., 2006;(Moreira et al., 2018) Bovi et al., 2020; Furlan et al., 2020).

2.2.2. Soil hydraulic conductivity

The soil hydraulic conductivity measurement method used in this research was an infiltration test with the demotion of water level, proposed by ABGE (2013). This soil permeability test is carried out in shal-

low holes and does not use a system for observing the piezometric loads around the holes; therefore, it is a one-off investigation that uses the measurement of sinking by time.

The permeameter consists of a 50 cm PVC tube, 9.6 cm inside diameter, and 10.2 cm outside diameter. In the tube, there is a transparent and graduated plastic window to measure the water level abasement.

The survey points were distributed following the geophysical lines: 100 m lines, orientation NW, and spacing of 15 m. The permeameter was fixed 10 cm deep in the soil. Altogether, there were 63 test points (Fig. 2).

Once the equipment was set, the tube was filled with water and left to saturate the ground for a certain period. The soil reached saturation when the readings of demotion the water level in the tube were repeated at least four times for a given time interval. It is considered a stabilized flow when no sudden variations in the read values are observed, the difference between isolated readings and the difference between the values does not exceed 20% (ABGE 2013). The following steps were followed: (i) the permeameter was filled with water in a column of 30 cm in height, configuring the time 0 s with 0 cm of the graduated rule; (ii) subsequent readings of demotion at 10 cm and 20 cm; (iii) the test is concluded when the abasement reaches 20% of the initial applied load.

2.2.3. Exploratory soil analysis

The auger soil surveys aimed to explore and characterize the soils of the study area. They also aimed to validate the data in the field and avoid ambiguities in understanding the geophysical and soil permeability data. The descriptions included texture, color (Munsell 2000), pedological features, and the presence of roots, moisture, and organic matter. We executed three points of auger surveys, all of them in the internal portion of the wetland (Fig. 2).

3. Results and discussion

3.1. Groundwater infiltration pattern

ERT data are presented in 2D inversion models with vertical elevation and horizontal distance in meters, with variable RMS adjustment between 6.4 and 12.4. This adjustment is consistent with the variation of the fixed values for all 2D inversion models in logarithmic scale between 50 Ω.m and 15,000 Ω.m, to allow comparisons between individual results (Fig. 3 and 4).

Line 1 was acquired at the western limit of the wetland and has characteristics of sandy soil developed in situ from sedimentary rocks: a thick layer of unsaturated soil/saprolite overlayed to a saturated layer correspondent to the perched water table (perched aquifer). The contact interface has a variable depth from 5 m to 7 m depth, possibly due to the proximity between the initial portion of the line and the wetland limit. In contrast, towards the end of the line, there is a growing distance from the wet area, accompanied by the deepness of the unsaturated soil/saprolite interface and the layered aquifer (Fig. 3).

Line 2 was acquired partly inside the wetland (initial half) and partly outside (final half) and has different characteristics from line 1 and similarities to other lines located inside the wetland. The initial half of the section presents a sloped zone of low resistivity (below 3000 Ω.m) which connects the land surface to a first horizontal layer that sequentially follows an inclination to deeper levels. This surface interval should represent a zone of higher infiltration of accumulated water during and after rain events, providing the direct recharge of perched water table (first horizontal layer below the recharge zone), which in turn allows the flow to the deeper aquifer (Fig. 3). The final half presents unsaturated soil/saprolite up to 8 m thick with a resistivity between 3000 Ω.m and 15,000 Ω.m.

Lines 3, 4, and 5 have similar elements, a unsaturated soil/saprolite horizon with a thickness between 2 m and 4 m with great lateral continuity and resistivity between 3000 Ω.m and 15,000 Ω.m. This portion is possibly segmented by resistivity intervals close to 3000 Ω.m. Below

this surface, there is a laterally continuous layer with a thickness ranging from 4 m to 6 m and resistivity between 500 Ω.m and 3000 Ω.m, with connection to the surface in lines 3 and 4. This layer should represent the local unconfined aquifer, with possible recharge zones due to infiltration of rainwater accumulated in the topographic depression, which crosses the horizon of soil/saprolite in the segmented intervals of low resistivity.

Below the unconfined aquifer, there is a layer with a thickness varying between 6 m and 14 m and resistivity between 3000 Ω.m and 4500 Ω.m, which acts as a substrate of low permeability and supports the unconfined aquifer, represented by sandstone with varying degrees of compaction and lithification, characterized as an aquitard. In the basal and central portion of the sections, there is a continuous layer beyond the depth of investigation of the lines, which presents resistivity values between 50 Ω.m and 3000 Ω.m, representing the top of the deep aquifer contained in porous and permeable sandstones. In this set of sections, there is no clear connection between shallow and deep aquifer.

In lines 3, 4, and 5 a discontinuous concretionary layer is identified in the soil cover represented by features with higher resistivities (6641–15,000 Ω.m) constituting sites that partially block rainwater and through lateral flow infiltrate faster in the iron-depleted sand soil matrices. Spatial differences in soil structures, bulk density, and textures result in differences in hydraulic characteristics flowing in large, continuous, structural pores (macropores) induced by an extreme discontinuity in permeability (Jarvis et al., 2007). A wide analysis of the data made it possible to delimit shallow or unconfined aquifer intervals, characterized by direct recharge by rainwater infiltration and positioned between layers of dry soil above and less permeable sandstone below. It was possible to recognize a connection between the unconfined aquifer and the deep aquifer. In the last case, layers of rock of high hydraulic conductivity allow the underground flow in a vertical direction (Figs. 3 and 4).

The elements highlighted for lines 3, 4, and 5 are also recurrent in lines 6, 7, 8, 9, and 10 (Fig. 4). In lines 7, 9, and 10, the dry soil/saprolite layer is segmented by areas of resistivity close to 3000 Ω.m and configure the unconfined aquifer recharge zones. In lines 6, 7, and 10 there is a continuous link between shallow and deep aquifer. Line 10 presents a resistivity zone greater than 15,000 Ω.m in the layer of water, which possibly represents a physiological variation within the sandstone layer, apparently of finer granulation and submitted to the same compaction and lithification regime as the other rock intervals, which resulted in an area of porosity and permeability lower than that predominant in this layer (Fig. 4).

3.2. Soil morphology and pedological features

Three auger surveys were performed to assess soil distribution, features, and validate the correspondence between electrical resistivity and hydraulic conductivity (Fig. 5).

Inside the wetland, Gleysol dominates with dismantled ferricrete in the subsurface. The hardness of iron crust and level of crust dissolution exerted influences on the results of resistivity and hydraulic conductivity (Fig. 5). In general, the soil profiles are highly sandy, resulted from the weathering and pedogenesis of sandstones of the Botucatu Formation. The soil matrices are composed of small (< 0.5 mm) washed grains of quartz, showing weak cohesion in a not developed structure (massive).

In the T1 profile, the clayey fraction slightly increases from the top to the bottom, and a weak-rounded substructure appears. The color change from grayish-brown (2.5Y 5/2) at 0–30 cm depth to yellowish-brown (10YR 5/8) at 70–220 cm. From 220 cm depth, ferruginous nodules dominate increasing in quantity, size, and resistance as far as the depth increases. The concretionary fragments are composed of coalescent purple and dark-red nodules associated with an indurated and more continuous layer of iron accumulation, which prevented the deepening of this survey (Fig. 5).

The T2 profile shows a similar sequence of soil layers, however, the concretionary layer occurs at greater depth (310 cm). From 0 to 70 cm,
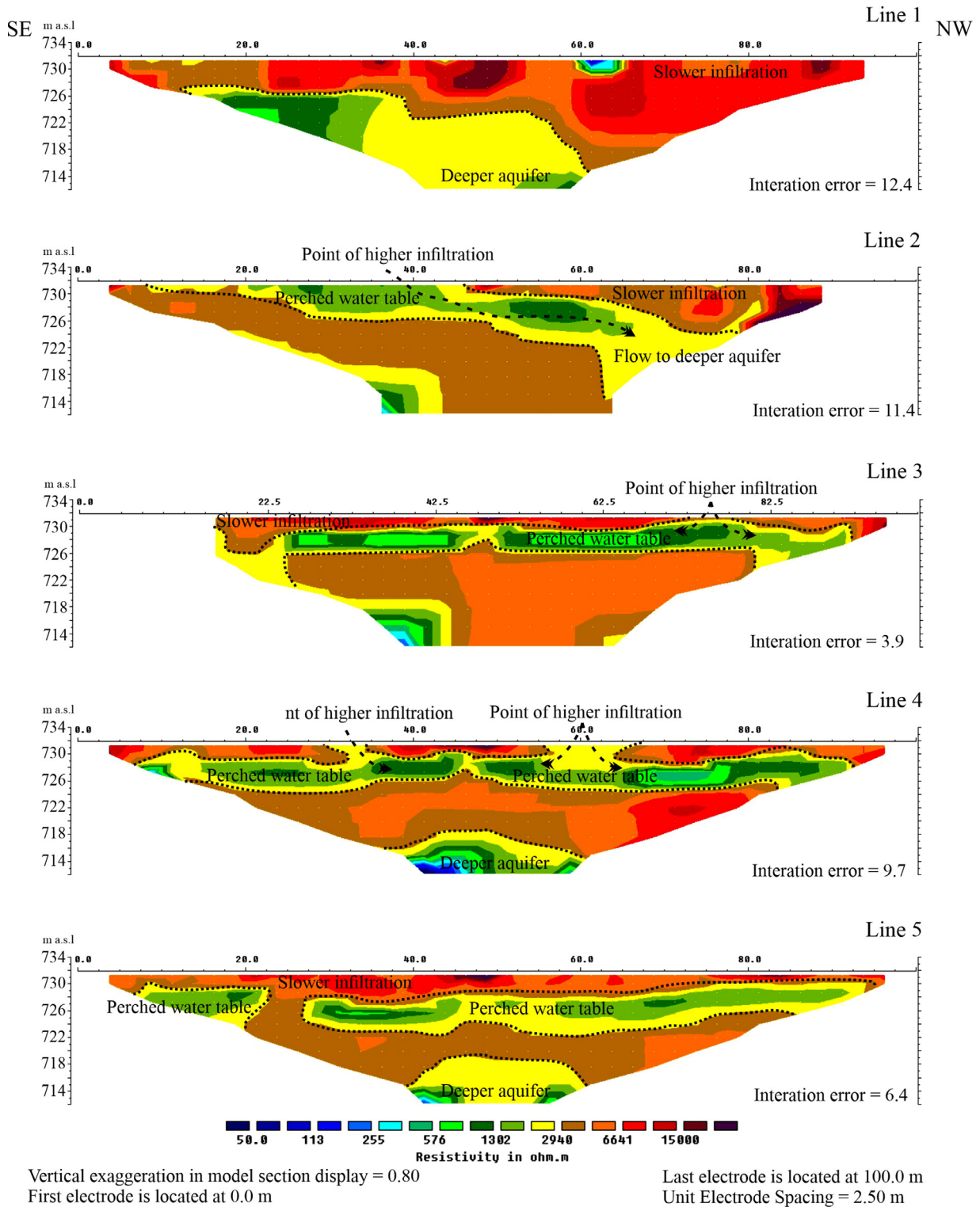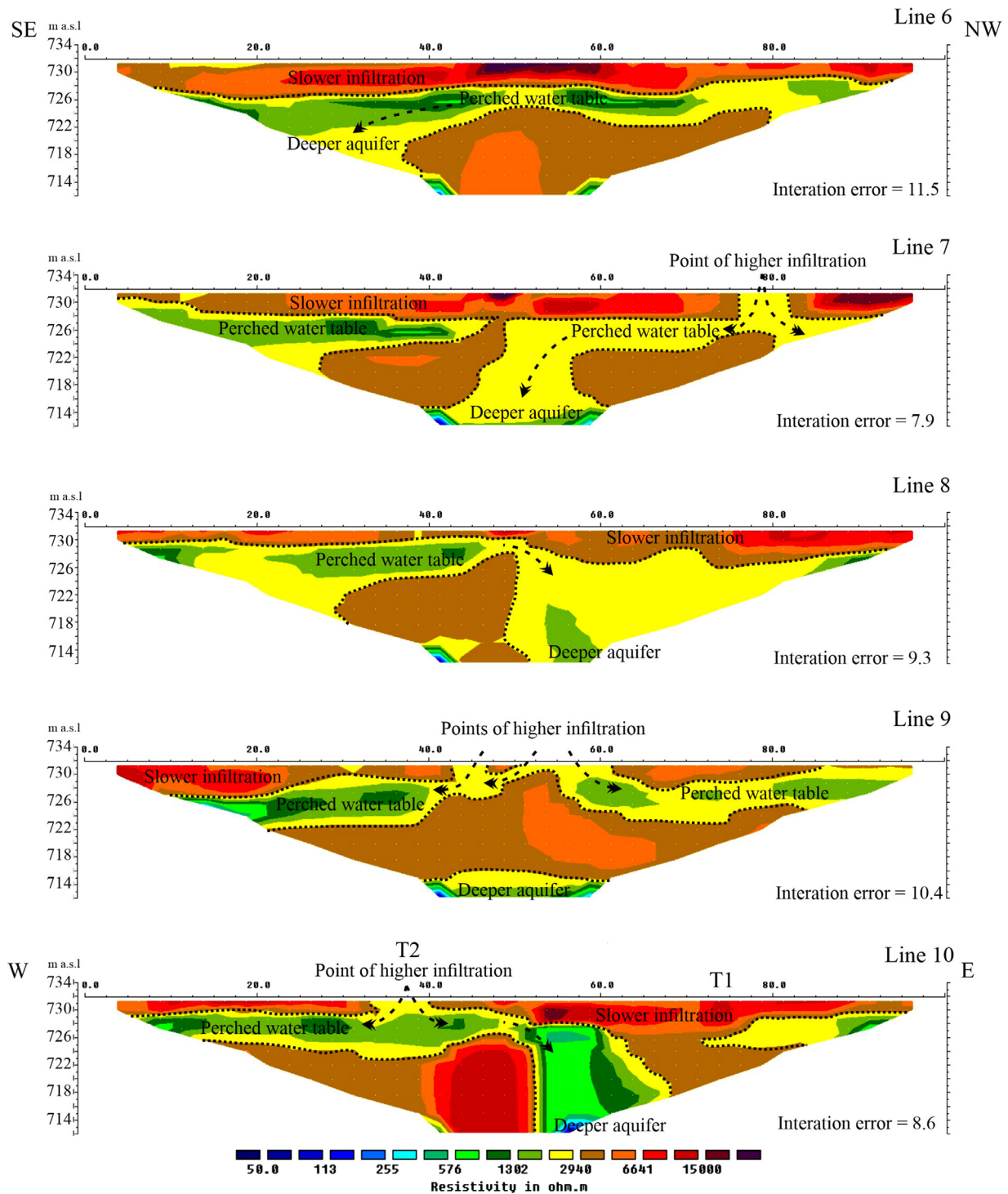
Fig. 3. Inversion models of ERT lines 1 to 5, highlighting the main structures of the local aquifer system.

the massive sandy horizons are light gray (2.5Y 7/2). The amount of clay fraction slightly increases from 70 to 270 cm. This mottled layer associates dark yellowish-brown and red spots (10YR 4/6 and 2.5YR 4/8) with dispersed hard ferruginous nodules (cm) with yellow goethite cortex indicating geochemical iron crust dissolution due to the increase of humidity (Tardy 1993). From 270 cm to 310 cm, quartz grains are strongly cemented by iron oxide in centimetric ferruginous concretions.

Due to the hardness of the substrate, it was not possible to advance to greater depths with a hand auger.

In the T3 profile, 0–60 cm depth the sandy texture is composed of washed grain quartz in a massive structure grayish-brown (2.5Y 5/2). From 60 to 250 cm occurs a slight increase of clay and the color is yellowish-brown (10YR 5/6). From 250 to 460 cm the soil matrices combine mottles dark yellowish brown (10YR 4/6) and dark red (2.5YR

Fig. 4. Inversion models of ERT lines 6 to 10, with highlighting the main structures of the local aquifer system.

3/4) with scarce, small, and friable iron nodules in the center of the spots (Fig. 5).

In Brazil, flat plateaus sustained by ferricrete are common under seasonal Savanna climate and the occurrence of a continuous hard layer can sustains a perched water table on the upper layers of soil cover. Since the surficial drainage is minor in the center of the plateau, the excess of water unbalances the link of iron oxides-clay, leaching some Fe and triggering internal pedological transformation generating the opening of

topographic concavities which advance to the plateau border (Lucas and Chauvel 1992). Local geomorphological and vegetation-related factors may have a strong influence on landscape and soil hydraulic evolution (Beerten et al., 2012). Generally, when lateritic ferruginous soil on a flat plateau is under hydromorphic conditions, shallow concavity develops on the top of the relief retaining rainwater in a temporary waterlogged environment. The process is well documented in the tropical region (Nahon 1991; Beauvais and Chardon 2013) and the accumulation of wa-
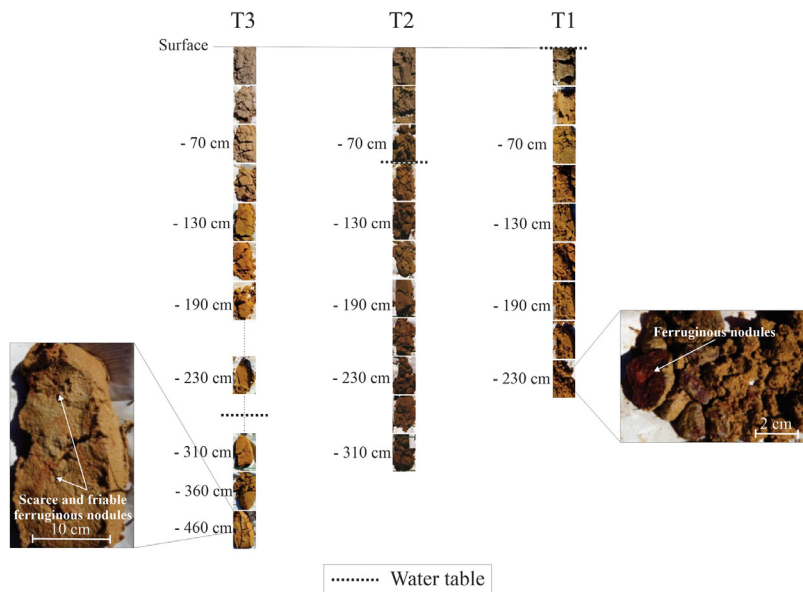
Fig. 5. Soil profiles sampled at points T1, T2 and T3. Zoom-in the depth with ferruginous nodules (T1) and scarce and friable ferruginous nodules (T3).

ter accelerates the continuous ferricrete dissolution because iron oxides became unstable and are released through soil solution (Vepraskas et al., 2012).

The studied soil profiles show heterogeneities in the level of laterite dissolution inside the wetland area suggesting a complex hydropedological system that can store rainwater on surface, where the ferricrete is more preserved (i.e., the T1 and T2 profiles), and increases vertical water flow where the ferricrete dissolution is higher (i.e., in the T3 profile). The distinction of surficial moisture reflects the sites where the surface water is retained for a longer time over more preserved ferricrete or interacts directly with the shallow aquifer having important implications on water dynamics and aquifer recharge. The ferricrete is no longer in equilibrium with the present landscape and the path opened by soil deferrugination can intensify the vertical flow of soil-water to greater depths reducing the periods of flooding. The transformation of ferricrete by iron-depletion under the present climate and its replacement by concretionary layer controls the moisture regime and the advance of the open Savanna over the water-resistant grass vegetation (Fig. 1B) (Mc Laughlin et al. 2014; Oliveira et al., 2017).

3.3. ERT survey integrated with soil hydraulic conductivity to evaluate the hydrogeology in the wetland

To improve the understanding of the groundwater flow and confirm the behavior and contribution of the wetland to the aquifer recharge, a pseudo-3D model was generated from the interpolation of all data generated by the 2D inversion. The result of the pseudo-3D was sliced and was generated maps of electric resistivity for depths −2 m, −4 m, and −9 m, to which the permeability map has been overlaid for a joint analysis (Fig. 6).

Although water infiltration occurs on the entire surface of the wetland, there are points with relatively higher or lower hydraulic conductivities. The resistivity maps were projected for a shared analysis with soil descriptions up to 2 m deep.

At T1 point, the soil was described in an area of relative lower permeability and high resistivity. This characteristic can be attributed to the presence of preserved ferricrete, which constitute a layer of low permeability, although this layer is overlayed between 0 m and −2 m by a sandy and well-drained material. It is possible that this hard lateritic horizon extended in a continuous layer of low permeability supporting a perched water table with a vertical extension up to 2 m. The mixture

of stored rainwater and the shallow perched water table submerges the land surface during the rainy season forming the wetland area.

The lateritic horizon recognized at point T1 represents a remnant of the iron crust and the opening of soil matrices facilitate the mixture of rainwater with perched water table as well as the increase of vertical flow toward the deeper aquifer. In contrast, the T2 soil profile correspond to an area of relative higher permeability and low resistivity, positioned in an area with an electrical resistivity of up to 3000 Ω.m, values that reflect a substantial increase in soil moisture compared to the area at T1 point. Therefore, this place shows higher infiltration rates and consequent recharge of the perched and deeper aquifer, whose development and expansion gradually reduces the capacity to maintain wetland (Fig. 6).

The T3 sampling point positioned in the limit of the wetland, coincides with intermediate values of hydraulic conductivity and high electrical resistivity, characterized by sandy soil at 2 m depth, continuous pattern up to the final depth of - 4.6 m, although with a slight increase in the content of clay minerals concomitant with increasing depth. T3 is where the soil profile indicates that the lateritic horizon presents an advanced stage of decomposition and dismantling, with strong deferruginization and substantial loss of water retention capacity (high resistivity values in depth).

Line 10 was positioned close to the soil sampling points T1 and T2. The integration of data allowed a detailed understanding of the relevance of the lateritic horizon in the waterproofing of the wetland substrate (Fig. 4).

Climate change and the establishment of warmer and wetter conditions between the end of the Pleistocene and during the Holocene induce the slow and natural degradation of lateritic surfaces in a tropical climate (Beauvais and Tardy 1993; Beauvais 1999; Beauvais et al., 1999; Horbe and Costa 2005;(Beauvais, 2009) Arruda et al., 2017; Rosolen et al., 2019), fundamental structure in the maintenance of several humid areas constituted by suspended aquifers, as described in several studies in Brazil (Rosolen et al., 2019; Furlan et al., 2020; Coelho et al. 2020).

Based on soil features, we assume that the expansion of the waterlogged area was higher when the cemented ferruginous crust was a continuous layer decreasing water permeability in the profiles. The advances of water accumulation amplify iron depletion diminishing the water saturation capacity even in the rainy periods. The increasing hydration and dissolution opened channels through which the water more
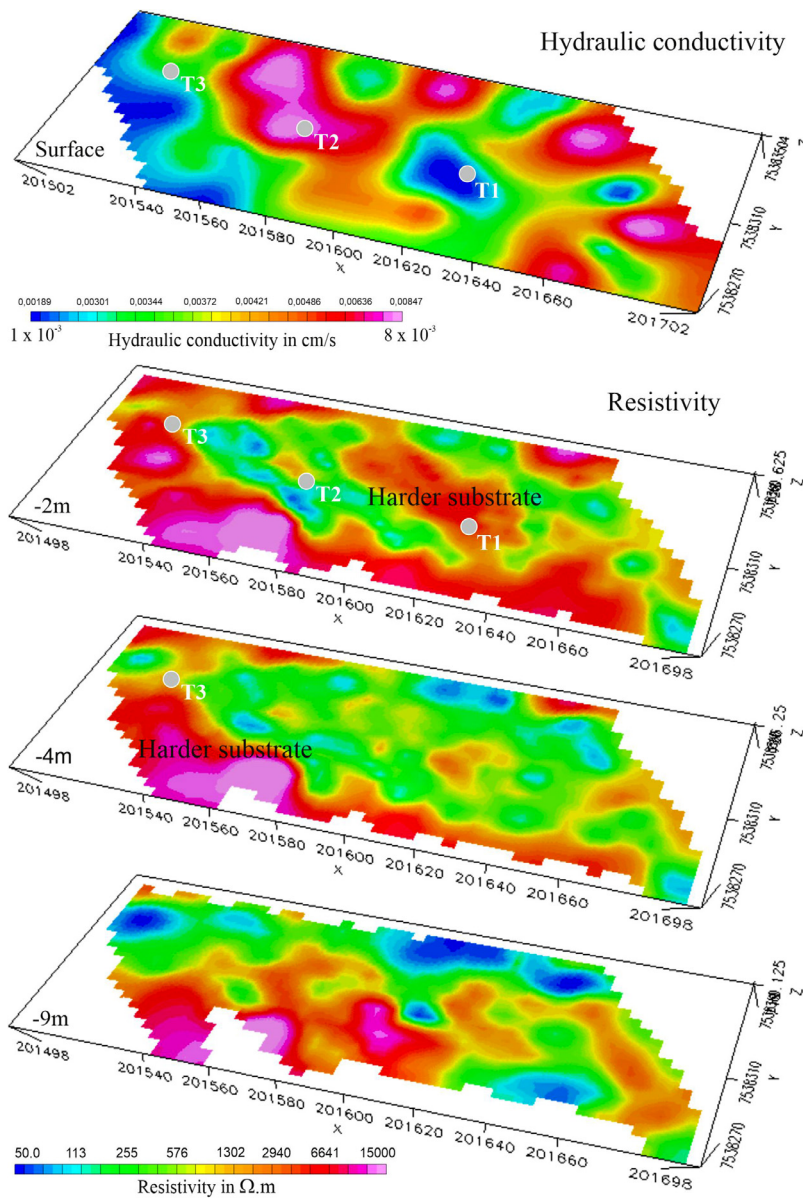
Fig. 6. Surface map of hydraulic conductivity, with the soil profiles' location, and maps of electric resistivity for depths 2 m, 4 m, and 9 m. The harder substrate portions are represented by the hot colors in the maps – 2 m (T1 and T3) and −4 m (T3).

easily flows vertically. Long-term in situ soil-water measures need to be carried out to evaluate the processes evolution in different hydroperiods.

On the other hand, the hydrological contribution capacity between wetland and other geomorphological compartments can be discussed. Although rainwater is the main source of the aquifer recharge, other conditions such as climatic variations, relief, soil, and rock permeability, the volume of precipitated water over time, and humidity are also fundamental factors (Sophocleous 2002; Marechal et al., 2008).

The configuration of relief and surface flow are fundamental factors even in sandy soils with high infiltration capacity, i.e., the slope favors surface runoff. Even in flat areas, the expulsion of the air contained in the soil pores requires time and long-term rains. The depression format of inland wetlands allows the accumulation of rainwater and the slow but constant infiltration into the soil, given the permanent existence of a saturated layer and the possibility of infiltration and recharge from short-term rains. This concept is detailed in Sophocleous (1991) and Sophocleous (2004).

Groundwater recharge should not be confused with water infiltration into the soil. The study by Custódio & Llamas (1976) distinguishes both processes. It states that the infiltration consists of the flow of surface

water to the unsaturated zone of the soil, while underground recharge represents the infiltrated volume that necessarily reaches the saturated zone of the soil and for deeper recharges. The flow paths recognized in 2D inversion models indicate the existence of complex systems within the wetland: existence of a perched watertable where the vertical flow is impeded, supported by a preserved lateritic horizon, with clear connection with the deeper aquifer.

Also, the water cycle in wetlands is strongly influenced by evapotranspiration. The study by Batista et al. (2018) describes the water balance in a hydrographic basin next to the study area, with the same geological and geomorphological context, to assess the influence of climate change on aquifer recharge and drainage discharge through isotopic analysis of the waters. The author found that the average annual precipitation is about 1453 mm and an evapotranspiration rate of about 940 mm; that is, almost 65% of rainwater returns to the atmosphere in a normal hydrological cycle of 12 months. The study also reveals that only rains above 200 mm provide a degree of soil saturation that can result in aquifer recharge.

Given the surface retention capacity of volumes below the minimum required for recharge, shallow perched water table can be defined as an

unconfined aquifer in the wetland area, that provide long periods of soil saturation and the possibility of connection with deeper aquifers. These elements indicate the great importance of the wetlands in the regional water balance.

Finally, worldwide, human activities have altered the volume and dynamics of water in wetlands. Intensive land use has negative consequences on river flows, and the relation with the wetland's hydroperiods are related in several countries in distinct geographical zones (Legesse et al., 2003; Tu 2009; Li et al., 2009; Tomer and Schilling 2009; Chen et al., 2013; (Santos et al., 2014); Onia et al., 2014).

4. Conclusion

This study has confirmed the behavior and contribution of inland wetland areas to aquifer recharge in the Savanna. By analyzing the 2D and pseudo-3D geophysical data integrated with soil descriptions and soil hydraulic conductivity, it was possible to trace the zones of higher water infiltration in the surface and determine a shallow water perched layer, connected with the groundwater aquifer system.

The perched aquifer is positioned between layers of lower hydraulic conductivity soil above and sandstone below. Layers of high permeability allow the groundwater flow in the vertical direction. There is a continuous link between shallow and deep aquifers, and the recharge zones occur due to infiltration of rainwater accumulated in the depression formed by the wetland.

The integration of data allows a detailed understanding of the relevance of the lateritic horizon (iron crust) in the waterlogging hydroperiods. This lateritic horizon originally constituted a wide layer of low hydraulic conductivity over the entire wetland area and acted as a support for the perched water table. A lateritic horizon in an advanced fragmentation reveals a large drainage area inside the wetland.

Author contributions

CAM and VR conceived and designed the study; all authors conducted data collection and processing; all authors wrote, read and approved the manuscript.

Declaration of Competing Interest

The authors declare that they have no known competing financial interests or personal relationships that could have appeared to influence the work reported in this paper.

Acknowledgments

References

ABEM. 2012. Terrameter LS instruction manual. ABEM instrument Sundbyberg: sundbyberg.

ABGE, 2013. Associação Brasileira de geologia de engenharia. Ensaios De Permeabilidade em Solos: Orientações Para a Sua Execução No Campo, 4th ed ABGE, São Paulo.

Alho, C.J.R., Martins, E.S., 1995. De Grao em Grao, o Cerrado Perde Espaco: Cerrado-Impactos do Processo de Ocupacao. Brasília: WWF-Fundo Mundial Para a Natureza, Brasília.

Almeida, F.F.M., 1964. Geological foundations of São Paulo relief. São Paulo: geographic and geological institute. Geol. State São Paulo 167–263.

Arruda, D.M., Schaefer, C.E.G.R., Fonseca, R.S., Solar, R.R.C., Fernandes-Filho, E.I., 2017. Vegetation cover of Brazil in the last 21 ka: new insights into the Amazonian refugia and Pleistocenic arc hypotheses. Glob. Ecol. Biogeogr. 27 (1), 47–56.

Batista, L.V., Gastmans, D., Sánchez-Murillo, R., Farinha, B.S., Santos, S.M.R., Kiang, C.H., 2018. Groundwater and surface water connectivity within the recharge area of Guarani aquifer system during El Niño 2014–2016. Hydrol. Process. 32 (16), 2483–2495.

Beauvais, A., Tardy, Y., 1993. Degradation and dismantling of iron crusts under climatic changes in Central Africa. Chem. Geol. 107 (3–4), 277–280.

Beauvais, A., 1999. Geochemical balance of lateritization processes and climatic signatures in weathering profiles overlain by ferricretes in Central Africa. Geochim. Cosmochim. Acta. 23/24, 3939–3957.

Beauvais, A., Ritz, M., Parisot, J.C., Dukhan, M., Bantsimba, C., 1999. Analysis of poorly stratified lateritic terrains overlying a granitic bedrock in West Africa, using 2-D. Earth Planet. Sci. Lett. 173 (4), 413–424.

Beauvais, Anicet, 2009. Ferricrete biochemical degradation on the rainforest–savannas boundary of Central African Republic. Geoderma 150, 379–388. doi:10.1016/j.geoderma.2009.02.023.

Beauvais, A., Chardon, D., 2013. Modes, tempo, and spatial variability of Cenozoic cratonic denudation: The West African example.. Geochem. Geophys. Geosyst. 14 (5), 1590–1608. doi:10.1002/ggge.20093.

Beerten, K., Deforce, K., Mallants, D., 2012. Landscape evolution and changes in soil hydraulic properties at the decadal, centennial and millennial scale: a case study from the Campine area, northern Belgium. Catena 95, 73–84.

Bovi, R.C., Moreira, C.A., Rosolen, V.S., Rosa, F.T.G., Furlan, L.M., Helene, L.P.I., 2020. Piping process: genesis and network characterization through a pedological and geophysical approach. Geoderma 361, 114101.

Bouwer, H., 2002. Artificial recharge of groundwater: hydrogeology and engineering. Hydrogeol. J. 10, 121–142.

Brannstrom, C., Jepson, W., Filippi, A.M., Redo, D., Xu, Z., Ganesh, S., 2008. Land change in the Brazilian Savanna (Cerrado), 1986–2002: comparative analysis and implications for land-use policy. Land Use Policy 25 (4), 579–595.

Carter, V., 1986. An overview of the hydrologic concerns related to wetlands in the United States. Can. J. Bot. 64 (2), 364–374.

Chen, X., Yang, X., Dong, X., Liu, E., 2013. Environmental changes in Chaohu Lake (southeast, China) since the mid-20th century: the interactive impacts of nutrients, hydrology and climate. Limnologica 43 (1), 10–17.

Custodio, E., Llamas, M.R., 1976. Hidrología Subterrânea. Omega, Barcelona.

Dahlin, T., 1996. 2D resistivity surveying for environmental and engineering applications. First Break 14 (7), 275–283.

de Vries, J., Simmers, I., 2002. Groundwater recharge: an overview of processes and challenges. Hydrogeol. J. 10, 5–17.

Farley, K.A., Jobbágy, E.G., Jackson, R.B., 2005. Effects of afforestation on water yield: a global synthesis with implications for policy. Glob. Change Biol. 11 (10), 1565–1576.

Fleischmann, A., Siqueira, V., Paris, A., Collischonn, W., 2018. Modelling hydrologic and hydrodynamic processes in basins with large semi-arid wetlands. J. Hydrol. 561, 943–959.

Fryirs, K.A., Wheaton, J.M., Bizzi, S., Williams, R., Brierley, G.J., 2019. To plug-in or not to plug-in? Geomorphic analysis of rivers using the River Styles Framework in an era of big data acquisition and automation. WIREs Water 6 (5), e1372.

Furlan, L.M., Rosolen, V., Sales, J., Moreira, C., Ferreira, M., Bueno, G., Mounier, S., 2020. Natural superficial water storage and aquifer recharge assessment in Brazilian savanna wetland using unmanned aerial vehicle and geophysical survey. J. Unmanned. Veh. Syst. 8 (3), 224–244.

Software, Geotomo, 2003. Res2Dinv (v.3.54) for 98/ME/2000/NT/XP. Geoelectrical Imaging 2D and 3D.

Hiscock, K.M., 2005. Hydrogeology: Principles and Practice. Blackwell Publishing, Oxford.

Horbe, A.M.C., Costa, M.L., 2005. Lateritic crusts and related soils in eastern Brazilian Amazonia. Geoderma 126, 225–239.

Jarvis, P., Rey, A., Petsikos, C., Wingate, L., Rayment, M., Pereira, J., Valentini, R., 2007. Drying and wetting of Mediterranean soils stimulates decomposition and carbon dioxide emission: the "Birch effect. Tree Physiol. 27 (7), 929–940.

Jepson, W., Brannstrom, C., Filippi, A., 2010. Access regimes and regional land change in the Brazilian Cerrado. 1972–2002. Ann. Assoc. Am. Geogr. 100, 87–111.

Junk, W., Piedade, M.T.F., Lourival, R., Wittmann, F., Kandus, P., Lacerda, L.D., Schöngart., J., 2014. Brazilian wetlands: their definition, delineation, and classification for research, sustainable management, and protection. Aquatic. Conserv. 24, 5–22.

Lee, S., Yeo, I.-.Y., Lang, M.W., Sadeghi, A.M., McCarty, G.W., Moglen, G.E., Evenson, G.R., 2018. Assessing the cumulative impacts of geographically isolated wetlands on watershed hydrology using the SWAT model coupled with improved wetland modules. J. Environ. Manage. 223, 37–48.

Legesse, D., Vallet-Coulomb, C., Gassea, F., 2003. Hydrological response of a catchment to climate and land use changes in Tropical Africa: case study South Central Ethiopia. J. Hydrol. 275 (1–2), 67–85.

Leite, M.B., Xavier, R.O., Oliveira, P.T.S., Silva, F.K.G., Matos, D.M.S., 2018. Groundwater depth as a constraint on the woody cover in a Neotropical Savanna. Plant Soil 426 (1), 1–15.

Li, L., Liu, W., Zhang, X., Zheng, F., 2009. Impacts of land use change and climate variability on hydrology in an agricultural catchment on the Loess Plateau of China. J. Hydrol. 377 (1–2), 35–42.

Loke, M.H., 2004. Tutorial: 2-D and 3-D Electrical Imaging Surveys. Geotomo Software www.geoelectrical.com.

Loke, M.H., Barker, R.D., 1996. Rapid least-squares inversion of apparent resistivity pseudosections by a quasi-Newton method. Geophys. Prospect. 44 (1), 131–152.

Lowrie, W., 2007. Fundamentals of Geophysics. Cambridge University Press, New York.

Lucas, Y., Chauvel, A., 1992. Soil Formation in Tropically Weathered Terrains. Handbook on Exploration Geochemistry, Regolith Exploration Geochemistry in Tropical and Subtropical Terrains. Elsevier, Amsterdam.

Marechal, J.C., Varma, M.R.R., Riotte, J., Vouillamoz, J.M., Kumar, M.S.M., Ruiz, L., Sekhar, M., Braun, J.J., 2008. Indirect and direct recharges in a tropical forested watershed: mule Hole. India. J. Hydrol. 364, 272–284.

Mawer, C., Parsekian, A., Pidlisecky, A., Knight, R., 2016. Characterizing Heterogeneity in Infiltration Rates During Managed Aquifer Recharge. Groundwater 54, 818–829.

Mclaughlin, D., Kaplan, D.A., Cohen, M.J., 2014. A significant nexus: geographic isolated wetlands influence landscape hydrology. Water Resour. Res. 50, 7153–7166.

Migoń, P., 2004. Etching, etchplain and etchplanation. In: Goudie, A.S. (Ed.), Encyclopedia of Geomorphology. Routledge, London, pp. 345–347.

Milani, E.J., Faccini, U.F., Scherer, C.M., Araújo, L.M., Cupertino, J.A., 1998. Sequences and stratigraphic hierarchy of the Paraná basin (Ordovician to Cretaceous), Southern Brazil. Boletim Inst. Geociênc./USP 29, 126–173.

Moreira, C.A., Paes, R.A.S., Ilha, L.M., Bittencourt, J.C., 2018. Reassessment of copper mineral occurrence through electrical tomography and pseudo 3D modeling in camaquã sedimentary basin. Southern Brazil. Pure Appl. Geophys. 176, 737–750.

Munsell, A.H., 2000. Munsell Soil Color Charts Munsell Color. GretagMacbeth, Michigan.

Mussett, A.E., Khan, M.A., 2000. Looking Into the Earth: An Introduction to Geological Geophysics. Cambridge University Press, New York.

Nahon, D.B., 1991. Self-organization in chemical lateritic weathering. Geoderma 51 (1–4), 5–13.

Nan, Y., Bao-hui, M., Chun-kun, L., 2011. Impact analysis of climate change on water resources. Procedia Eng. 24, 643–648.

Nosetto, M., Jobbágy, D., Brizuela, E.G., Jackson, A.B., 2012. The hydrologic consequences of land cover change in central Argentina. Agric. Ecosyst. Environ. 154 (1), 2–11.

Oliveira, P.T.S., Leite, M.B., Mattos, T., Nearing, M.A., Scott, R.L., de Oliveira Xavier, R., Wendland, E., 2017. Groundwater recharge decrease with increased vegetation density in the Brazilian cerrado. Ecohydrology 10 (1), 1759.

Onia, S.K., Futter, M.N., Molot, L.A., Dillon, P.J., Crossman, J., 2014. Uncertainty assessments and hydrological implications of climate change in two adjacent agricultural catchments of a rapidly urbanizing watershed. Sci. Total Environ. 473-474 (1), 326–337.

Robineau, B., Join L., J., Beauvais, A., Parisot C., J., Savin, C., 2006. Geoelectrical imaging of a thick regolith developed on ultramafic rocks: groundwater influence. Aust. J. Earth Sci. 773–781. doi:10.1080/08120090701305277.

Rosolen, V.S., Bueno, G.T., Mutema, M., Moreira, C.A., Faria Junior, I.R., Nogueira, G., Chaplot, V., 2019. On the link between soil hydromorphy and geomorphological development in the Cerrado (Brazil) wetlands. Catena 176, 197–208.

Salazar, A., Baldi, G., Hirota, M., Syktus, J., McAlpine, C., 2015. Land use and land cover change impacts on the regional climate of non-Amazonian South America: a review. Glob. Planet. Change 128, 103–119.

Sano, E.E., Rosa, R., Brito, J.L.S., Ferreira, L.G., 2010. Land cover mapping of the tropical savanna region in Brazil. Environ. Monit. Assess. 166, 113–124.

Santos, R.M.B., Sanches Fernandes, L.F., Moura, J.P., Pereira, M.G., Pacheco, F.A.L., 2014. The impact of climate change, human interference, scale and modeling uncertainties on the estimation of aquifer properties and river flow components. J. Hydrol. 519, 1297–1314.

Schneider, R., Mühlmann, H., Tommasi, E., Medeiros, R.D., Daemon, R.F., Nogueira, A.A., 1974. Revisão estratigráfica da Bacia do Paraná. In XXVIII Congresso Brasileiro de Geologia (Porto Alegre), 28, 41–66.

Sendrós, A., Himi, M., Lovera, R., Rivero, L., Garcia-Artigas, R., Urruela, A., Casas, A., 2020. ERTmonitoring of two managed aquifer recharge ponds in the alluvial aquifer of the Llobregat River (Barcelona, Spain). Near Surf. Geophys. 18, 353–368.

Sonkamble, S., Sahya, A., Jampani, M., Ahmed, S., Amerasinghe, P., 2019. Hydro – geophysical characterization ans performance evaluation of natural wetlands in a semi-arid wasterwater irrigated landscape. Water Res. 148, 176–187.

Sophocleous, M., 2002. Interactions between groundwater and surface water: the state of the art. Hydrogeol. J. 10 (1), 52–67.

Sophocleous, M., 2004. Global and regional water availability and demand: prospects for the future. Nat. Resour. Res. 13 (2), 61–75.

Sophocleous, M.A., 1991. Combining the soilwater balance and water-level fluctuation methods to estimate natural groundwater recharge: practical aspects. J. Hydrol. 124 (3–4), 229–241.

Tardy, Y., 1993. Pètrologie des Laterites et des Sols Tropicaux. Masson, Paris.

Telford, W.M., Geldart, L.P., Sheriff, R.E., 1990. Applied Geophysics. Cambridge University Press, Cambridge.

Tomer, M.D., Schilling, K.E., 2009. A simple approach to distinguish land-use and climate-change effects on watershed hydrology. J. Hydrol. 376 (1–2), 24–33.

Troppmair, H., 2000. Geossistemas e Geossistemas Paulistas. Helmut Troppmair, Rio Claro.

Tu, J., 2009. Combined impact of climate and land use changes on streamflow and water quality in eastern Massachusetts. USA.J. Hydrol. 379 (3–4), 268–283.

Van der Kamp, G., Hayashi, M., 1998. The groundwater recharge function of small wetlands in the semi-arid Northern Prairie. Gt. Plains Res. 8, 39–56.

Vepraskas, M.J., Lindbo, D.L., Lin, H., 2012. Redoximorphic Features As Related to Soil Hydrology and Hydric Soils. Hydropedology: Synergistic Integration of Soil Science and Hydrology. Henry Lin ed. Academic Press, San Diego.

Whigham, D.F., Jordan, T.E., 2003. Isolated wetlands and water quality. Wetlands 23 (3), 541–549.

Winter, T.C., 1999. Relation of streams, lakes, and wetlands to groundwater flow systems. Hydrogeol. J. 7, 28–45.

Zanchetta, D., Diniz, F.V., 2006. Estudo da contaminação biológica por Pinus spp. em três diferentes áreas na Estação Ecológica de Itirapina (SP, Brasil). Rev. Inst. Flor. 18, 1–14.